

Recent US advances in ion-beam-driven high energy density physics and heavy ion fusion [☆]

B.G. Logan^{a,*}, F.M. Bieniosek^a, C.M. Celata^a, J. Coleman^a, W. Greenway^a, E. Henestroza^a, J.W. Kwan^a, E.P. Lee^a, M. Leitner^a, P.K. Roy^a, P.A. Seidl^a, J.-L. Vay^a, W.L. Waldron^a, S.S. Yu^a, J.J. Barnard^b, R.H. Cohen^b, A. Friedman^b, D.P. Grote^b, M. Kireeff Covo^b, A.W. Molvik^b, S.M. Lund^b, W.R. Meier^b, W. Sharp^b, R.C. Davidson^c, P.C. Efthimion^c, E.P. Gilson^c, L. Grisham^c, I.D. Kaganovich^c, H. Qin^c, A.B. Sefkow^c, E.A. Startsev^c, D. Welch^d, C. Olson^e

^aLawrence Berkeley National Laboratory, 1 Cyclotron Road, MS47R0112, Berkeley, CA 94720-8210, USA

^bLawrence Livermore National Laboratory, Livermore, CA 94550, USA

^cPrinceton Plasma Physics Laboratory, Princeton, NJ 08543-0451, USA

^dVoss Scientific, Albuquerque, NM 87108, USA

^eSandia National Laboratories, Albuquerque, NM 87185, USA

Available online 28 February 2007

Abstract

During the past two years, significant experimental and theoretical progress has been made in the US heavy ion fusion science program in longitudinal beam compression, ion-beam-driven warm dense matter, beam acceleration, high brightness beam transport, and advanced theory and numerical simulations. Innovations in longitudinal compression of intense ion beams by $>50X$ propagating through background plasma enable initial beam target experiments in warm dense matter to begin within the next two years. We are assessing how these new techniques might apply to heavy ion fusion drivers for inertial fusion energy.

© 2007 Elsevier B.V. All rights reserved.

PACS: 41.75.Ak; 52.20.Mj; 29.27.—a

Keywords: Heavy ion beams; Neutralized plasma; Inertial fusion; Beam compression

1. Introduction

This paper describes research on compressing heavy ion beams towards the high intensities required for creating high energy density matter and inertial fusion energy. In previous research, experiments [1] and simulations [2] showed $>100X$ increases in focused beam intensities in the Neutralized

Transport Experiment by transverse compression of an intense ion beam propagating through a background plasma to neutralize $>90\%$ of the beam space charge. Section 2 describes recent work on longitudinal compression of an intense beam within neutralizing plasma, and in Section 3 we describe studies of initial warm dense matter target experiments that can be enabled after transverse and longitudinal beam compression are combined. Progress in testing a novel Pulse Line Ion Accelerator (PLIA) is described in Section 4, e-cloud experiments, theory and simulations in Section 5, advanced injectors in Section 6, and advanced theory and simulation models in Section 7. Section 8 discusses potential applications to heavy ion fusion drivers, and conclusions are given in Section 9.

[☆]This research was performed under the auspices of the US Department of Energy by the University of California, Lawrence Berkeley and Lawrence Livermore National Laboratories under Contract Numbers DE-AC02-05CH11231 and W-7405-Eng-48, and by the Princeton Plasma Physics Laboratory under Contract Number DE-AC02-76CH03073.

*Corresponding author. Tel.: +1 510 486 7206; fax: +1 510 486 5392.

E-mail address: bglogan@lbl.gov (B.G. Logan).

2. Neutralized drift compression

Our approach to maximize both beam energy deposition and heating uniformity is to place the peak in ion beam dE/dx at the center of thin targets (a few microns' thickness, corresponding to the range of MeV ion beams) [3]. Such thin targets will hydro-expand in a few nanoseconds at 1 eV temperature, so short pulses of a few ns are needed instead of the few μ s pulses previously used. Longitudinal compression of an ion bunch using a velocity ramp head-to-tail while traveling through neutralizing background plasma provides a means of generating ion beam pulses short enough to be consistent with the hydro expansion time of few-micron-thick target foils for near-term warm dense matter physics experiments.

In the Neutralized Drift Compression Experiment [4] (NDCX-*Fig. 1*), an induction core adds a velocity ramp from the head to the tail of a selected 200–400 ns portion of a 20–25 mA, 300 kV K^+ ion beam. The induction core consists of 14 pancake-shaped cores of magnetic material that add up the voltages from 14 separately adjustable primary input voltage pulses to provide tailored voltage ramps to the ion beam bunch passing through. An induction voltage ramp of approximately ± 100 kV amplitude is applied to the beam, and is shaped to provide a nearly linear (as linear as possible) head-to-tail velocity ramp for longitudinal compression. The amplitude of the velocity ramp is sufficient to allow the rear of the selected beam slice to catch up with ions in the head of the slice over a 1.3-m drift section that is pre-filled with plasma confined in a weak solenoid magnetic field. The drift compression section provides space charge neutralization during axial compression.

We tuned the 14 separate induction cores to optimize the compressing induction voltage waveforms to achieve the

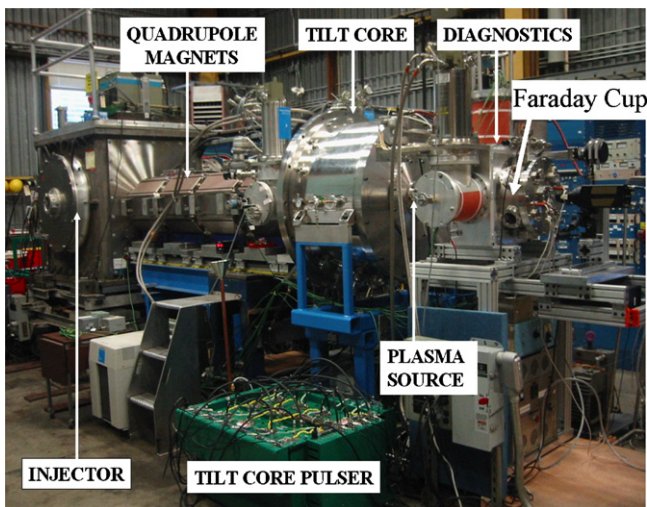


Fig. 1. The new NDCX-1A facility began operation in December 2004. The facility utilizes the injector from the previous NTX experiment, together with an induction “tilt” core (center), to induce a velocity ramp to compress the beam. There is also a longer plasma-filled drift tube between the tilt core and the end diagnostics, compared to NTX.

maximum longitudinal bunch compression of 60X [5], measured with a fast (ns-response) Faraday cup and an optical beam scintillator. When the 3D particle-in-cell simulations [6,7] used the actual measured induction input waveforms in modeling the induction buncher, we were able to achieve excellent agreement between measured and simulated compression of the total beam current (*Fig. 2*). No significant loss of beam current is observed so that peak currents of over an ampere are observed in the compressed pulse, when starting with an injected current of 20 mA. Notably, signs of any beam plasma instabilities such as two-stream are not observed, and are also not seen in the simulations that can resolve such instabilities. A longitudinal beam temperature $T_z < 1.5$ eV is measured with an improved-resolution electrostatic energy analyzer, which is consistent with the low longitudinal beam temperatures that simulations require in order to explain the large compression factors that are achieved. A longitudinal beam temperature of 1.5 eV is higher than the expected source temperature, but is consistent with the degree to which the actual induction voltage waveform does not provide exactly linear velocity ramps, suggesting further improvements in the induction waveform and peak compressions are possible. A longer plasma source [8] will be tested soon to optimize neutralization of beams [9] over a greater range of distances and velocity ramps.

3. Design of experimental ion-beam-driven warm dense matter target experiments

Over the last year we have evaluated an initial set of ion-beam-heated experiments [10,11] to contribute to the science of warm dense matter as expeditiously as possible using modest improvements [12] to present beam facilities (NDCX and HCX). The list of experiments below is planned to yield scientifically interesting results at progressively higher beam intensities and increasing target temperatures.

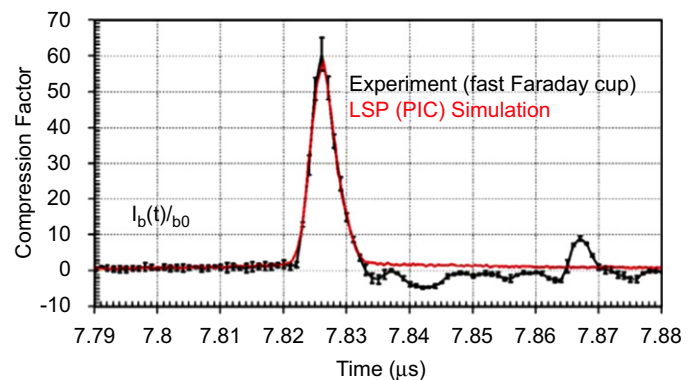


Fig. 2. Comparison of fast Faraday cup current waveform with LSP PIC simulations for an NDCX compression experiment. When the actual, experimentally realized waveforms were inserted in the simulations (red curve), good agreement with the data is seen. (See papers by Seidl, et al., Sefkow, and Welch, these proceedings.)

a. Beam-induced transient emission and absorption experiments in transparent insulators (on HCX and NDCX): The beam excites electrons to higher energy states, resulting in a darkening of the otherwise transparent material. The goal is to corroborate the understanding of the phenomena that have been observed at higher temperatures.

b. Experiment to measure target temperature and conductivity using a beam compressed both transversely and longitudinally (on NDCX): Here the best focus (both longitudinally and transversely) that can be obtained on the present NDCX experiment will be used to raise the target temperature as high as possible, and begin to make hydrodynamic and conductivity experiments.

c. Positive–negative halogen ion plasma experiment ($kT > \sim 0.4 \text{ eV}$) [13] (on NDCX with focusing solenoid, or pulse compressed HCX with focusing solenoid): The conductivity of such a novel plasma composed primarily of positive and negative ions may be similar to that of semi-conductors at high densities.

d. Two-phase liquid–vapor metal experiments ($kT > 0.5\text{--}1 \text{ eV}$) (on NDCX with focusing solenoid or pulse compressed HCX with focusing solenoid or NDCX-upgraded): The exact phase transition boundary for a number of metals is unknown and the dynamics passing through this phase is also important to determine.

e. Critical point measurements ($kT > 1 \text{ eV}$) (possibly only on NDCX-upgraded): The critical point occurs at the highest temperature for which a distinction between the gaseous and liquid state can be observed.

In addition, it is planned to carry out metallic foam heating experiments at GSI that will begin to explore the physics of foam targets as well as possible measurements of dE/dX in metallic foam. Ion stopping may be different when the time between collisions is less than the relaxation timescale of the ion in the excited state.

4. Pulse Line Ion Accelerator (PLIA)

The first acceleration of non-relativistic K^+ ion bunches with a helical slow wave structure immersed in a coaxial dielectric (PLIA [14], Fig. 3) has been demonstrated. Due to the traveling wave that provides the accelerating field, significant energy amplification has been achieved with modest voltage pulses. Depending on the phase of ions with respect to the traveling wave, a beam energy modulation of $-80\text{--}+150 \text{ keV}$ on the NDCX beam was measured using a PLIA input voltage waveform of $-21\text{--}+12 \text{ kV}$. The resulting beam energy modulation is consistent with WARP simulations (Fig. 4). We are currently studying the causes and possible remedies of a vacuum breakdown that presently limits $\langle E_z \rangle < 150 \text{ kV/m}$ [15]. If we can achieve high gradients through continuing modeling and experiments, the PLIA may greatly reduce the cost per volt for accelerators used to heat target experiments using ions near the peak of dE/dx .

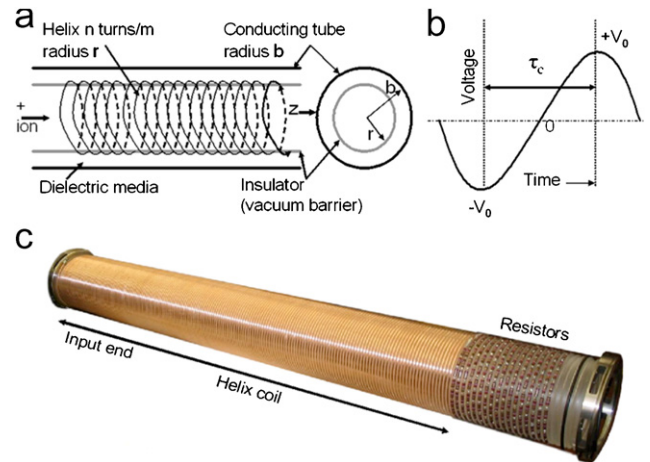


Fig. 3. A schematic of the helical pulse line structure. (a) The helical pulse line of radius r is located inside a conducting cylinder of radius b , and a dielectric medium is located in the region outside the helix; (b) schematic of a drive voltage waveform applied at the helix input; and (c) a 1-m-long helix constructed for the PLIA experiments.

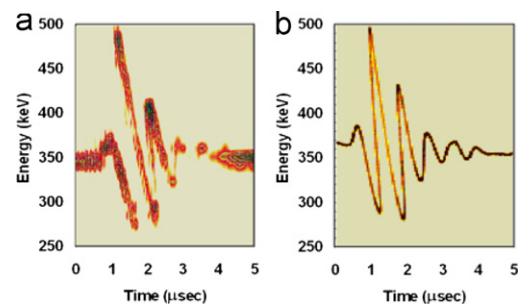


Fig. 4. The energy distribution (measured with a new energy analyzer) of NDCX K^+ beam ions accelerated through a 1 m PLIA section (Fig. 1). The measured ion output energies (a) are modulated depending on the ion phase with respect to the ringing waveform. WARP-3D simulations (b) reproduce the measured energy modulation. (See papers by Roy, Henestroza, and Coleman, these proceedings).

5. High brightness beam transport

In any accelerator with high intensity, positively charged beams, the beam space potential can attract and trap secondary electrons from beam–wall interactions, or electrons from ionization of background gas. When the associated electron clouds build up sufficiently to substantially reduce the net beam space charge, the beam transport itself can be affected, and non-linearities in the net beam charge due to electron clouds can cause degradation of the beam brightness. We have refined electron-cloud and gas experiments in the High Current Experiment (HCX) with improved diagnostics [16] and models [17]. We made the first absolute measurement of e-cloud densities [18], and increased the understanding of electron emission. An important source of electrons is from emission induced by ions impacting the beam tube near grazing incidence. We have measured the electron emission coefficient and angle of incidence dependence for ions from 50 keV to 1 MeV [19].

The trapping of electrons within an ion beam in a four-quadrupole magnet system [18] has been studied. A suppressor ring electrode (at the exit of the four-quadrupole system) and clearing electrodes (positively biased rings inserted into the drift regions between quadrupole magnets) provide the knobs to control electron flow from the end wall and pipe wall into the beam region. Trapped electrons reduce the net beam potential by partial neutralization, which we measure with a new diagnostic, the retarding field analyzer (RFA). A small number of cold ions are generated within the beam by beam-impact ionization of the background gas, and subsequently expelled by the net beam potential. The energy distributions of expelled ions are measured, from which we determine the peak potential of the beam, and its variation over the beam pulse.

We find significant agreement between measured and simulated e-cloud effects on a high current ion beam transported through four quadrupole magnets in HCX. As in the beam compression experiments in NDCX discussed above, advanced simulations also closely support the e-cloud experiments in HCX. Fig. 5 shows a snapshot of electron density in a simulation of the HCX beam being substantially neutralized in the last magnet from secondary electrons drifting in from the end wall on the right [20]. These simulations are made possible by a large time-step particle mover that allows us to simulate complex electron drifts in 3D magnetic fields. Fig. 5 exhibits large amplitude (\sim beam space charge density level) oscillations in the electron cloud at 6 MHz, consistent in frequency and amplitude with those measured. We are beginning to test these e-cloud models in solenoid transport experiments in

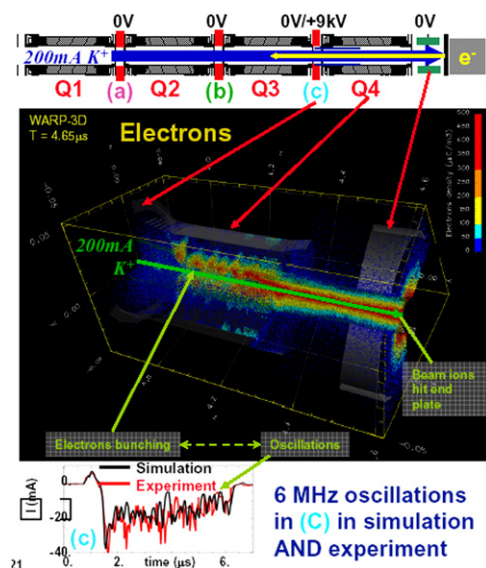


Fig. 5. Top: four HCX magnetic quadrupoles with clearing electrodes at (a), (b) and (c). Middle: the charge density of primary electrons (color coded) simulated from emission off the beam hitting the end wall on the right, and extending from through the last magnet to the clearing electrode between the last two magnets. Bottom: overlay of measured and simulated 6 MHz e-cloud oscillations in location (c).

NDCX (Fig. 6), so that we can compare e-cloud effects in solenoids as well as in quadrupoles. A predictive e-cloud capability is important to design future accelerators using high intensity positively charged beams.

6. Advanced theory and simulation tools

Advanced theory and simulations have improved our understanding of the collective stability properties of intense heavy ion beams and beam–plasma interactions, and of multi-species interactions with gas and strong electron “clouds” affecting intense beam transport [21–24]. Strongly anisotropic beams may be subject to electrostatic Harris-type instability [25], which may increase the parallel beam temperature and thus may inhibit subsequent longitudinal neutralized drift compression. Collective processes of an intense ion beam with charge-neutralizing background plasma, such as the electrostatic two-stream instability, the electromagnetic multi-species Weibel instability, and the resistive hose instability [24,26] may also affect ultimate focusing of compressed neutralized beams. Conditions minimizing deleterious effects of collective processes on beam quality have been identified [27].



Two-solenoid NDCX Transport Experiment

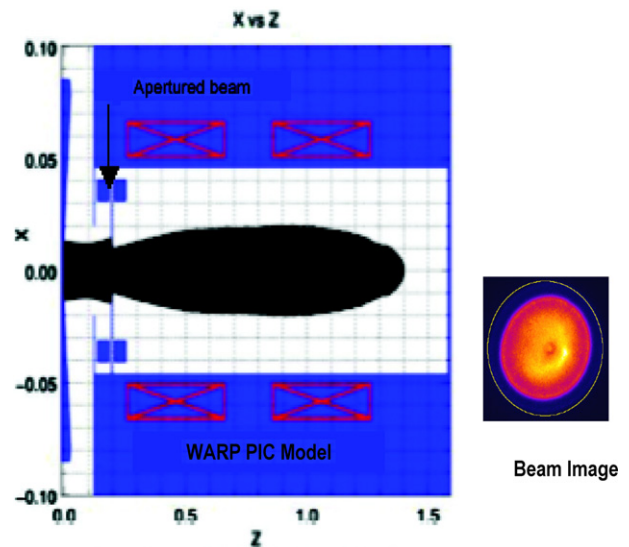


Fig. 6. Initial solenoid transport experiment in NDCX using a 25 mA, 300 keV K^+ ion beam in two 3T solenoids. The WARP PIC simulation agrees with measurements near the beam head (within the first microsecond). At later times, the beam envelope shrinks while current is observed on an electron suppressor ring at the end, possibly due to gas/e-cloud buildup. More diagnostics and modeling are planned to clarify e-cloud and gas effects on transport in four solenoids.

Our simulation tools for treating interaction of intense ion beams in accelerators with gas and electron cloud effects have seen considerable development over the past several years. This progress has enabled studies of the new regimes required for high energy density physics and warm dense matter studies. The tools and numerical techniques are also proving very useful for a broad range of accelerator physics and particle trap applications. A comprehensive set of models [28] governing the interaction of positively charged beams with electron clouds (e-clouds) and gas has been developed and implemented in the WARP code. Secondary electron emission from walls, charge exchange, neutral emission, and other processes are now included. The package encapsulates several important plasma–wall interaction physics effects. Fig. 7 shows how the various plasma wall interactions relate to one another.

7. Development of advanced injectors

The Converging-Beamlets Experiment on the 500-kV test stand at LLNL (STS-500) was successfully completed in 2005 [29]. In operation up to 400 keV beam energy at the designed beam current of near 80 mA, the beam pulses were reproducible without voltage breakdown issues. Simulations using WARP3d were used to design the experiments, and results are in good agreement with simulations [30]. This concluded after several years of effort in the development of an advanced, compact, low cost high-current injector for heavy ion fusion drivers. This experiment has validated the multi-beamlet injector concept, producing high brightness, high-current beams using a very compact injector. It establishes a new injector option for heavy ion accelerators, such as modular solenoid and multiple-beam induction linacs. This approach also allows potential use of high power ECR plasma sources [31] of higher charge state ions such as Ar^{+8} , which is especially important in the context of modular HIF drivers that require high currents of high charge-to-mass-ratio ions, in

order to lower the cost and boost the efficiency of single-beam solenoid-focused linacs.

8. Studies of neutralized drift compression applied to heavy ion fusion drivers

Studies of the application of neutralized beam compression and focusing (NDC) to heavy ion fusion linac drivers have continued since 2004. The primary benefit of removing space charge during drift compression and focusing is expected to be allowed the use of higher charge-to-mass ratio ions to reduce linac voltage, length and cost, when the beam perveance would be otherwise too high to drift compress and focus in vacuum. In 2004, systems analysis [32] found that use of 200 MeV Ne^{+1} with NDC could potentially reduce 6.4 MJ driver costs by about a factor of about two, for both a multiple-beam quadrupole-focused single induction linac driver (MQ driver) as well as for a driver system of 24 modular, single-beam solenoid-focused induction linacs (MS driver), under the assumption that suitable injectors and final focus/chamber designs can be developed. Recent improvements in high-voltage induction cells [33] have allowed DARHT-II to become one of the largest induction linacs operating in the world, now undergoing scaled beam acceleration tests. Later this year, DARHT-II will test fast downstream kicker magnets for multi-pulsing kA electron beams, and this technology is relevant to time-dependent chromatic error corrections. There are several issues remaining to be assessed, including high brightness, high-current injectors of high q/A ions, electron cloud effects in the linacs, and chromatic focusing errors due to coherent velocity ramps for compression of neutralized bunches.

Recently, studies have considered injection, transport, and focusing of ions with $q/A > 0.1$ [34], and also with use of NDC with fast time-dependent kickers to compensate focusing errors due to coherent velocity ramps as large as 10% and with > 200 mrad focusing angles. Results are encouraging, but these are still works in progress. We also anticipate that if we can make beam focal spots below 1 mm, then we may be able to access heavy ion fusion targets having requisite gains of 40 with total driver energies as low as 1 MJ [34]. Assuming injector and final focusing studies will find conceptual solutions for injection and focusing high q/A ions for 1 MJ drivers, and assuming e-cloud effects can be controlled, we have meanwhile used modified versions of the IBEAM systems code [35] to make additional assessments of potential reductions in linac mass (here mass is a surrogate for cost) for MQ and MS driver cases. Recent development of high-current ECR sources of high charge state Argon ions [31] should enable injectors for Ar^{+8} . Fig. 8 shows cross-sections of 1 MJ heavy ion driver examples, one based on a scaled-down MQ driver for Bi^{+1} ions otherwise similar to the Robust Point Design (RPD) [36], the other a cross-section for an example MS driver using Ar^{+8} . The MQ example could use RPD-style injectors and focusing, while the MS driver example shown

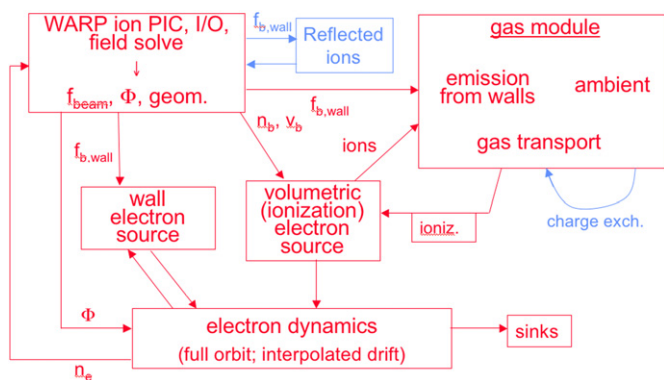


Fig. 7. We have almost completed the implementations of all of the modules in the roadmap for developing self-consistent modeling of electron and gas cloud effects in high intensity ion accelerators. (Implemented modules are in red; those undergoing implementation are in blue.) See papers by Cohen and Vay, these proceedings.

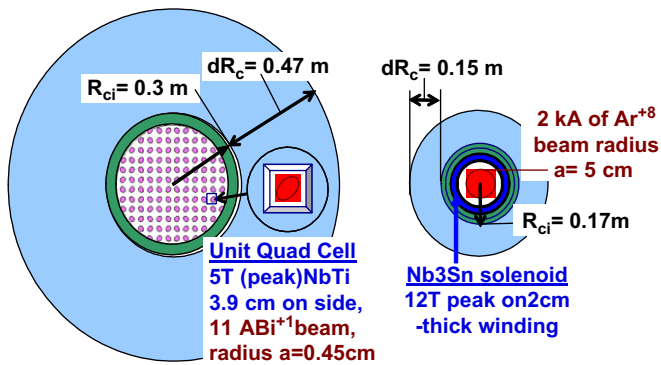


Fig. 8. Comparing HIF linac driver example cross-sections: Left: Multi-beam Quad (MQ) driver, an RPD-like design [13] scaled down to produce 1 MJ of 4 GeV Bi^+ ions in a single pulse. Right: Modular Solenoid (MS) driver system, one of 40 linacs, to produce 1 MJ total of 500 MeV Ar^{+8} with five pulses per linac.

in Fig. 8 takes advantage of NDC together with time-dependent compensation of coherent velocity ramps to overlap 5 sequential bunches during drift compression to the target. Other parameters from the IBEAM systems analysis for the two examples shown in Fig. 8 are given in Table 1 under the columns labeled “Low q/A MQ” and “High q/A MS”, along with another case “High q/A MQ” that optimizes an MQ driver with Ar^{+8} with three sequential pulses in a manner similar to the high q/A MS driver case with 5 pulses. For reference, the original RPD driver design for 7.6 MJ targets [36] had a total induction magnetic material (cores) mass of 35,600 tons. The 1 MJ low q/A MQ driver case in Table 1 shows a weak scaling of MQ driver cost with energy with low q/A ions, namely, the 1 MJ Bi^+ MQ driver has $\frac{2}{3}$ of the total core mass of the 7.6 MJ RPD. In contrast, by using NDC with multiple pulses of high q/A (Ar^{+8}) ions, the linac lengths and core masses for both high q/A MQ and MS driver cases are reduced about an order of magnitude from the low q/A MQ case. One particular challenge in the high q/A MQ example is the need to build very small 4 T quadrupole magnets of length 9 cm and radius 2.6 cm with 7 mm clearance between the beam and pipe radii, to limit phase advance per half-lattice period to less than 80° for Ar^{+8} ions.

There are other critical needs to address. All driver cases optimized with the IBEAM systems code neglect e-cloud effects, so effective means must be found to virtually eliminate e-cloud effects in the acceleration regions of all cases. A key motivation for the e-cloud studies described in Section 5 comparing both solenoidal and quadrupole magnetic geometries is to evaluate the efficacy of methods to mitigate e-cloud effects in those geometries, and to be able to model small residual e-cloud effects on the beam brightness. This knowledge is essential to permit future integrated studies of both MQ and MS HIF driver approaches including various mitigation effects such as axial electron kicks in induction gaps. All induction driver cases require longitudinal bunch compression by factors of

Table 1

Comparison of 1 MJ HIF drivers based on a modified IBEAM systems code (no-e-cloud)

Driver type	Low q/A MQ Bi^+	Hi q/A MQ Ar^{+8}	Hi q/A MS Ar^{+8}
E_{total} (MJ)	1	1	1
# Pulses	1	3	5
# Linacs	1	1	40
# Bunches	120×1	150×3	40×5
Range (g/cm^2)	0.03	0.03	0.03
$T_{i\text{max}}$ (MeV)	4000	600	600
$T_{i\text{min}}$ (MeV)	3300	500	500
Voltage (MV)	4000	75	75
Length (m)	2900	300 ^a	75×40
$I_{\text{injection}}$ (A)	0.075	5.2	12
I_{final} (A)	11	176	2000
Cores (tons)	21,400	1930	2400
Efficiency ^b	0.21	0.55	0.28

MQ = multiple beam magnetic quad linac. MS = modular solenoid linac system.

^aIncludes 160 m ESQ section to 100 MeV.

^bBased on core losses only.

5 to 10X during initial acceleration between injection and the main linac. Both the high q/A MQ and MS driver cases need multiple pulses to achieve shorter bunch durations, so as to get reasonable induction gradients together with core masses low enough for efficiencies $>25\%$, which requires fast, efficient, and low-cost solid state switching. The output bunch train lengths of 50 and 40 m for the 3-pulse MQ and 5-pulse MS driver cases require 500 to 400 m-long NDC sections, respectively, assuming 10% velocity ramps and chromatic error compensation between the head and tail bunches to allow the bunches to converge at the target. The detailed convergence timing should be controlled to provide the required target pulse shaping (an advantage over one-pulse linacs). An important development path advantage of the MS approach over the MQ approach is that a driver prototype can be validated with one linac module at full ion energy with $<3\%$ of the high q/A MQ linac mass.

9. Conclusions

The present and planned research should provide the physics knowledge base needed to optimize the design of future heavy ion accelerators for both high energy density physics and heavy ion fusion energy drivers, including both multiple-beam quadrupole-focused linac and modular solenoid-focused linac development path options towards inertial fusion energy.

References

- [1] P.K. Roy, S.S. Yu, S. Eylon, E. Henestroza, A. Anders, E.P. Gilson, F.M. Bieniosek, W.G. Greenway, B.G. Logan, W.L. Waldron, D.B. Shuman, D.L. Vanecek, D.R. Welch, D.V. Rose, C. Thoma, R.C. Davidson, P.C. Efthimion, I. Kaganovich, A.B. Sefkow, W.M. Sharp, Nucl. Instr. and Meth. Phys. Res. A544 (2005) 225.

- [2] C. Thoma, D.R. Welch, S.S. Yu, E. Henestroza, P.K. Roy, S. Eylon, E.P. Gilson, *Phys. Plasmas* 12 (2005) 043102.
- [3] L.R. Grisham, *Phys. Plasmas* 11 (2004) 5727.
- [4] P.K. Roy, S.S. Yu, E. Henestroza, A. Anders, F.M. Bieniosek, J. Coleman, S. Eylon, W.G. Greenway, M. Leitner, B.G. Logan, W.L. Waldron, D.R. Welch, C. Thoma, A.B. Sefkow, E.P. Gilson, P.C. Efthimion, Davidson, *Phys. Rev. Lett.* 95 (2005) 234801.
- [5] P.K. Roy, et al., *Nucl. Instr. and Meth. A* (2007), doi:10.1016/j.nima.2007.02.056.
- [6] A.B. Sefkow, R.C. Davidson, P.C. Efthimion, E.P. Gilson, S.S. Yu, P.K. Roy, F.M. Bieniosek, J.E. Coleman, S. Eylon, W.G. Greenway, E. Henestroza, J.W. Kwan, D.L. Vanecsek, W.L. Waldron, D.R. Welch, *Phys. Rev. ST Accel. Beams* 9 (2006) 052801.
- [7] D.R. Welch, et al., *Nucl. Instr. and Meth. A* (2007), doi:10.1016/j.nima.2007.02.057.
- [8] P.C. Efthimion, et al., *Nucl. Instr. and Meth. A* (2007), doi:10.1016/j.nima.2007.02.088.
- [9] I.D. Kaganovich, et al., *Nucl. Instr. and Meth. A* (2007), doi:10.1016/j.nima.2007.02.039.
- [10] J.J. Barnard, et al., *Nucl. Instr. and Meth. A* (2007), doi:10.1016/j.nima.2007.02.062.
- [11] F.M. Bieniosek, et al., *Nucl. Instr. and Meth. A* (2007), doi:10.1016/j.nima.2007.02.063.
- [12] A. Sefkow, et al., *Nucl. Instr. and Meth. A* (2007), doi:10.1016/j.nima.2007.02.064.
- [13] L.R. Grisham, et al., *Nucl. Instr. and Meth. A* (2007), doi:10.1016/j.nima.2007.02.061.
- [14] R.J. Briggs, et al., Helical pulse line structure for ion acceleration, in: *Proceedings of the 2005 Particle Accelerator Conference, IEEE, Piscataway, NJ, 2005* (<http://accelconf.web.cern.ch/accelconf/>).
- [15] J.E. Coleman, et al., *Nucl. Instr. and Meth. A* (2007), doi:10.1016/j.nima.2007.02.053.
- [16] A.W. Molvik, et al., *Nucl. Instr. and Meth. A* 544 (2005) 194.
- [17] R.H. Cohen, et al., *Nucl. Instr. and Meth. A* (2007), doi:10.1016/j.nima.2007.02.035.
- [18] M. Kireeff Covo, et al., *Phys. Rev. Lett.* 97 (2006) 054801.
- [19] M. Kireeff Covo, et al., *Phys. Rev. ST-AB* 9 (2006) 063201.
- [20] J.-L. Vay, et al., *Nucl. Instr. and Meth. A* (2007), doi:10.1016/j.nima.2007.02.013.
- [21] A. Friedman, *Nucl. Instr. and Meth. A* (2007), doi:10.1016/j.nima.2007.02.010.
- [22] R.C. Davidson, I. Kaganovich, H. Qin, E.A. Startsev, D.R. Welch, D.V. Rose, H.S. Uhm, *Phys. Rev. ST Accel. Beams* 7 (2004) 114801.
- [23] H. Qin, et al., *Nucl. Instr. and Meth. A* (2007), doi:10.1016/j.nima.2007.02.038.
- [24] H. Qin, R.C. Davidson, E.A. Startsev, *Phys. Rev. ST Accel. Beams* 6 (2003) 014401.
- [25] E.A. Startsev, R.C. Davidson, H. Qin, *Phys. Rev. ST Accel. Beams* 8 (2005) 124201.
- [26] R.C. Davidson, et al., *Nucl. Instr. and Meth. A* (2007), doi:10.1016/j.nima.2007.02.036.
- [27] E.A. Startsev, et al., *Nucl. Instr. and Meth. A* (2007), doi:10.1016/j.nima.2007.02.037.
- [28] J.-L. Vay, M.A. Furman, R.H. Cohen, A. Friedman, D.P. Grote, A. W. Molvik, P. Stoltz, S. Veitzer, J. Verboncoeur, Filling in the roadmap for self-consistent electron cloud and gas modeling, in: *Proceedings of the 2005 Particle Accelerator Conference, IEEE, Piscataway, NJ, 2005*, (<http://accelconf.web.cern.ch/accelconf/>).
- [29] G.A. Westenskow, et al., *Nucl. Instr. and Meth. A* (2007), doi.org/10.1016/j.nima.2007.02.050.
- [30] D.P. Grote, et al., *Nucl. Instr. and Meth. A* (2007), doi:10.1016/j.nima.2007.02.012.
- [31] S.V. Golubev, S.V. Razin, V.G. Zorin, *Rev. Sci. Inst.* 69 (1998) 634.
- [32] W.R. Meier, B.G. Logan, *Nucl. Instr. and Meth. A* 544 (2005) 310.
- [33] B.A. Prichard, Jr., J. Barraza, M. Kang, K. Nielson, F. Bieniosek, K. Chow, W. Fawley, E. Henestroza, L. Reginato, W. Waldron, R. Briggs, T. Hughes, T. Genoni, Technological improvements in the DARHT-II accelerator cells, in: *Proceedings of the 2005 Particle Accelerator Conference, IEEE, Piscataway, NJ 2005*, (<http://accelconf.web.cern.ch/accelconf/>).
- [34] D.A. Callahan-Miller, M. Tabak, *Phys. Plasmas* 7 (2000) 2083.
- [35] W. Meier, R. Bangerter, J. Barnard, *Nucl. Instr. and Meth. A* 464 (2001) 433.
- [36] S.S. Yu, W.R. Meier, R.P. Abbott, J.J. Barnard, T. Brown, D.A. Callahan, P. Heitzenroeder, J.F. Latkowski, B.G. Logan, S.J. Pemberton, P.F. Peterson, D.V. Rose, G.-L. Sabbi, W.M. Sharp, D.R. Welch, *Fusion Sci. Technol.* 44 (2003) 266.